

AN ILLUSTRATION OF THE ADVANTAGES OF A COMPLETE TEXTURE ANALYSIS DESCRIBED BY THE ORIENTATION DISTRIBUTION FUNCTION (ODF) USING QUARTZ POLE FIGURE DATA

S.M. SCHMID¹, M. CASEY¹ and J. STARKEY²

¹ *Geologisches Institut der E.T.H., Zurich (Switzerland)*

² *Geological Department, University of Western Ontario, London, Ont. (Canada)*

(Received January 26, 1981)

ABSTRACT

Schmid, S.M., Casey, M. and Starkey, J., 1981. An illustration of the advantages of a complete texture analysis described by the orientation distribution function (ODF) using quartz pole figure data. In: G.S. Lister, H.-J. Behr, K. Weber and H.J. Zwart (Editors), *The Effect of Deformation on Rocks*. *Tectonophysics*, 78: 101–117.

The preferred orientation of eight crystal directions of quartz was measured with an X-ray texture goniometer for selected quartz-bearing tectonites with a clear pattern of *c*-axis preferred orientation. The advantages of data analysis by means of calculations of the orientation distribution function and other forms of data presentation derived from the ODF are demonstrated.

INTRODUCTION

In naturally deformed rocks the relationship between the ease of deformation on the various slip systems along a given deformation path and the resulting texture is not immediately obvious. Experiments to determine the relevant slip systems, and computer simulations allowing for a more complex deformation path than can be achieved experimentally are necessary. So far the analyses of natural textures have been largely restricted to the incomplete information gained from considering one crystal direction (the *c*-axis) alone. A limited number of complete texture analyses of quartz are available; Baker and Wenk (1972), Bunge and Wenk (1977), Riekels and Baker (1977) and Bouchez et al. (1979) presented such analyses in the form of orientation distribution functions (ODF), a method of data presentation used for some time by metallurgists (Bunge, 1969). The results of computer simulations (Lister et al., 1978) have been presented in the form of *c*-axis pole figures and inverse pole figures only. A representation of the results in the form of

an ODF would be possible but was not undertaken because of the difficulties in including the effects of Dauphinée twinning in the simulation process (G.S. Lister, pers. commun., 1980).

The present contribution aims towards a better understanding of the complete crystal preferred orientation for some tectonites with simple and characteristic *c*-axis preferred orientations. Interpretations are advanced where possible. The specimens selected illustrate the advantages of this rather complicated technique of data presentation. Thereby it is hoped to stimulate further analyses of this kind and also to provide a more complete basis for comparison with computer simulations.

METHODS OF DATA COLLECTION AND ANALYSIS

For each specimen eight pole figures were measured with an automatic X-ray texture goniometer (Seiffert-Scintag) operating in combined reflection and transmission mode (Siddans, 1976). The intensities were measured along a step scan with 5-degree intervals in both azimuth and tilt angle of a given specimen direction. By choosing 40 sec counting time for each position on the pole figure and 100 sec for two background positions measured once for every small circle at constant angle of tilt, one pole figure could be measured per day. The eight reflections used in this study are shown in the crystal projection of Fig. 1. Equivalent positive and negative forms cannot be analyzed separately. The relative intensity contributions of positive and negative forms used for the calculation of the ODF were obtained from the structure factors measured by Smith and Alexander (1963).

For the data processing we used a set of FORTRAN computer programs developed and described by Casey (1981, this volume) and for details the reader is referred to this companion paper and also to Bunge (1969). A description of the Eulerian angle convention used in this study is also given in Casey (this volume). Readers unfamiliar with the data presentation in the form of an ODF are referred to Bunge and Wenk (1977) for an extensive description and to Schmid et al. (1981) for a concise introduction.

MICROSTRUCTURE AND GEOLOGICAL SETTING OF THE SPECIMENS

Four specimens described below were chosen to illustrate complete texture analysis. In the descriptions use is made of finite-strain terminology to identify planes and directions in the specimen. This terminology conflicts with the convention for the specimen coordinate system given by Casey (this volume). In finite-strain terminology the *X*-direction is the axis of greatest extension and *Z* is the axis of greatest shortening, taken to be parallel to stretching lineation of foliation normal respectively. It is convenient to have the *Y*-axis of finite strain in the centre of the pole figure.

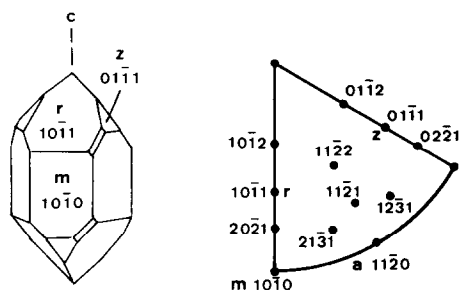


Fig. 1. Model of right-handed quartz and equal area projection of the poles to the diffracting planes used for the X-ray texture analysis.

GAE 9

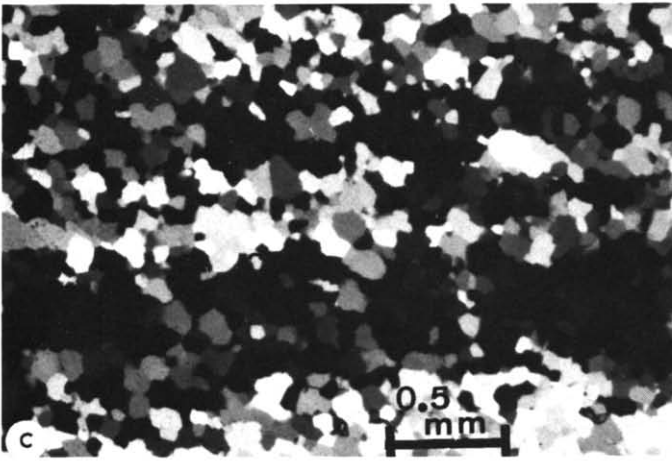
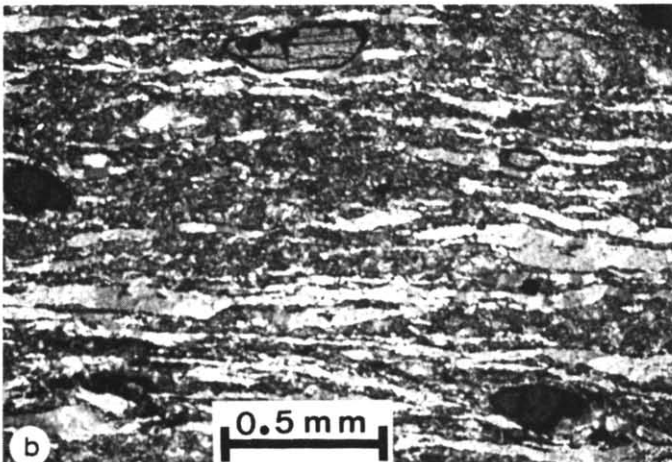
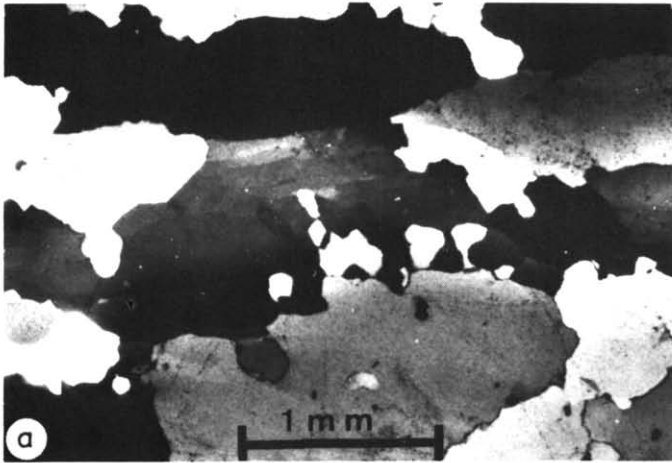
This quartzite of sedimentary origin was collected from the limb of a gigantic syncline in the Sierra de Caurel, Galicia, by Ph. Matte (Montpellier). A regional description of the area is found in Matte (1968). The rock was deformed under upper amphibolite facies conditions. Foliation and lineation are defined by elongate quartz grains in the XZ -section as well as in the XY -section (Fig. 2a). The foliation is additionally marked by a preferred alignment of minor amounts of white micas and deviates by 15° from the only macroscopically visible bedding planes in an anticlockwise sense in reference to the projection of Fig. 3c. The grain size varies between 0.25 and 2 mm which is rather coarse for an X-ray texture analysis.

GRAN 133

Saxony granulite from the Tirschheim borehole at a depth of 20 m (Behr 1965). Figure 2b illustrates that quartz constitutes only a fraction of the rock volume and that although the rock is lineated, the high aspect ratio of the quartz aggregates in this section perpendicular to the lineation indicates a strong component of flattening. All minerals other than quartz were exsolved using a silica saturated hydrofluoric acid (Kerrick and Starkey, 1979). The grain size of quartz is around 25–50 μm . Behr (1961, 1965) ascribed the textures of the granulites to having formed under amphibolite facies conditions overprinting the earlier granulite facies.

CC 627 and CC 550

Quartzite veins from the centres of shear zones in Cap de Creus, Spain, described by Carreras et al. (1977). The rocks were deformed under green-



schist facies conditions. The grain size of around $100\ \mu\text{m}$ is very uniform and the grains are equant (Fig. 2c). The well equilibrated grain boundaries are indicative of dynamic recrystallization by a subgrain rotation mechanism. Figure 2c also shows a banding parallel to the foliation caused by domains which have a similar orientation: the light areas have their *c*-axes at a high angle to the *Y*-direction in the centre of the pole figure (Fig. 3c) whereas the dark areas remain dark during rotation of the section under crossed polarizers indicating that they consist of grains with their *c*-axis predominantly close to the *Y*-direction. The sense of shear in both specimens as indicated in Figs. 3c and 7 has been deduced from the sense of the shear zone in the field, the lineation lies near the shear direction.

RESULTS

Figure 3 shows that both specimens GAE 9 and GRAN 133 have a *c*-axis point maximum. Whereas this point maximum lies near the lineation for GAE 9, it is parallel to the intermediate strain axis *Y* in GRAN 133. GRAN 133 has been represented in a *YZ*-section in order to make comparisons with GAE 9 easier.

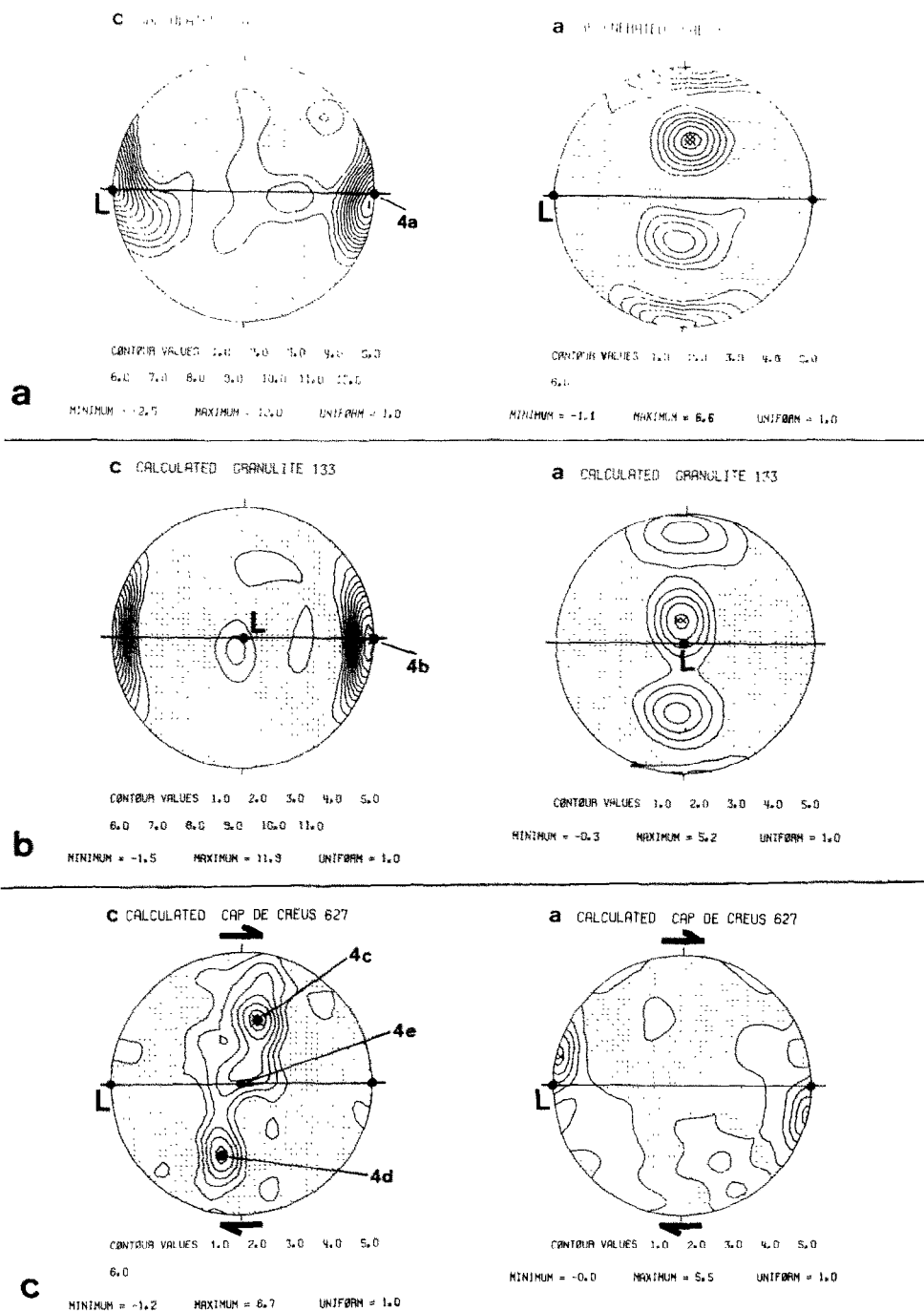
Specimen CC 627 has the *c*-axes along a girdle which is oblique at $10\text{--}20^\circ$ to the foliation normal. This deviation from parallelism with the macroscopic fabric axes is consistent with the sense of shear of the shear zone as inferred from field studies.

The *a*-axis pole figures of both GAE 9 and GRAN 133 exhibit a very simple pattern (Fig. 3) indicating that there is an extremely good preferred orientation of these second-order prisms into three maxima 60° apart and corresponding to their positions in a single crystal. In GAE 9 one *a*-maximum is parallel to the foliation normal whereas in GRAN 133 the *a*-maximum deviates by 15° from the foliation normal. This places the foliation normal between the maxima for first- and second-order prisms *m* and *a*.

Specimen CC 627 exhibits a strong single maximum of *a* poles 15° away from the lineation (Fig. 3c), close to the pole of the *c*-axis girdle.

It is clear that this additional information cannot be predicted from the *c*-axis pole figure alone, but so far these simple textures could be quite adequately described without performing a calculation of the orientation distribution function. Figure 4, however, contains additional information which

Fig. 2. a. Photomicrograph of specimen GAE 9 in the plane of the foliation and with the lineation E–W. Note the deformation bands oriented subparallel to the lineation and grain boundary bulging indicative of strain-induced grain-boundary migration.
 b. Specimen GRAN 133 cut perpendicular to both foliation and lineation. Quartz is restricted to the light coloured elongate bands often only one grain broad.
 c. Specimen CC 627 cut perpendicular to foliation and with the lineation E–W. The light and dark areas are domains with similar *c*-axis orientations at low and high angles to the plane of the section, respectively. The sense of shear is sinistral for this micrograph.



Pole figures for *c* and *a*, calculated from the ODF. Foliation trace E-W;
L=Lineation

Fig. 3. Pole figures for *c* and *a* (1120), calculated from the ODF, order of expansion 12. The labels 4a-e refer to the *c*-axis positions corresponding to the profiles in Fig. 4. a-e. Foliation traces E-W; lineation E-W for specimens GAE 9 (Fig. 3a) and CC 627 (Fig. 3c), in the centre of the pole figure for GRAN 133 (Fig. 3b). Contour intervals in 1.0 of a uniform distribution, stippled areas with a density < 1, equal area projection.

can only be extracted from an ODF. The profiles of this figure indicate the probabilities of finding crystal directions other than the c -axis direction in a given orientation and they refer to fixed positions of the c -axis, defined by PSI 1 and PHI, indicated in the c -axis pole figure of Fig. 3. From these profiles we extract the following information:

The otherwise similar textures of GAE 9 and GRAN 133 are different in respect to the preferred orientation of positive and negative forms. In GRAN 133 the probability of finding a pole to a positive form in a given specimen direction is nearly equal to the probability for the pole to the corresponding negative form (equal intensities for positions 60° apart along PSI 2). This "hexagonal" character of the texture is indicated by the two peaks of the same strength. Specimen GAE 9, however, is characterized by two peaks of

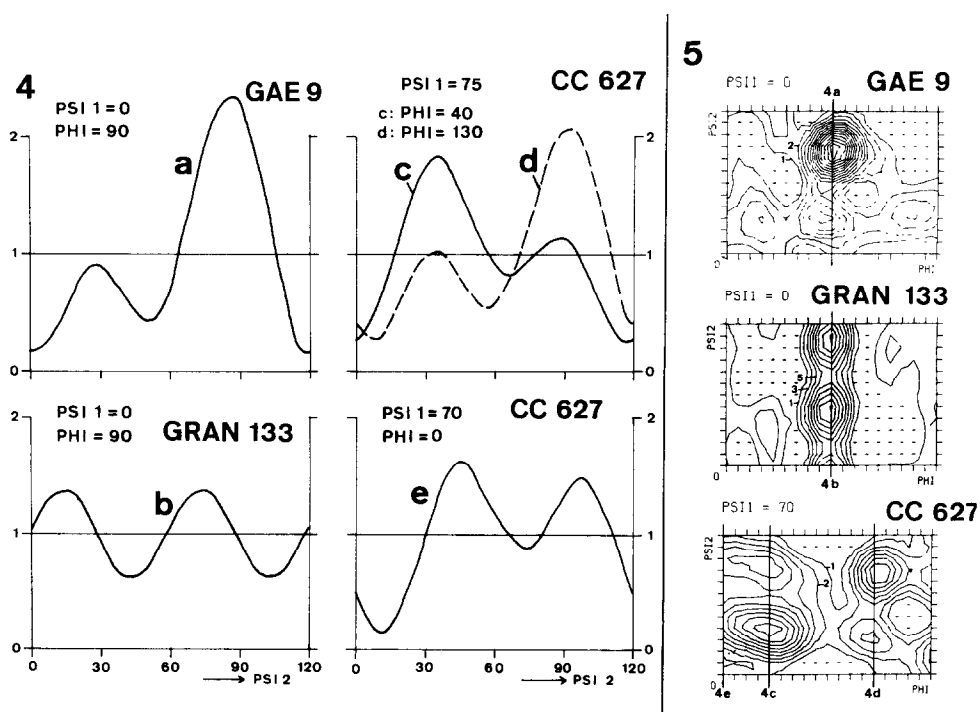


Fig. 4. Renormalized intensity profiles, indicating the nature and degree of a preferred orientation of lattice directions other than the c -axis in terms of a profile along PSI 2 (rotation around the final position of the c -axis) for the c -axis positions indicated in Figs. 3 and 5.

Fig. 5. Sections through the ODF in the PSI 2 - PHI plane at constant angle PSI 1, order of expansion 8. These selected sections contain information about all the crystals with c -axis in an E-W trace through the pole figures in the case of specimens GAE 9 and GRAN 133 (PSI 1 = 0) and in a NNE-SSW trace in the case of specimen CC 627 (PSI 1 = 70). Dashes indicate crystal positions with probabilities calculated to be negative.

very unequal strength, i.e. the texture discriminates between positive and negative forms.

For specimen CC 627 three *c*-axis positions were chosen for this profile representation: two of the profiles (Fig. 4, *c* and *d*), corresponding to the *c*-axis maximum positions, exhibit two peaks of unequal strength whereas we find two peaks of nearly equal strength for the *c*-axis position in the centre of the pole figure. This illustrates the interdependence between *c*-axis position and the character of the preferred orientation of positive and negative forms.

The profiles of Fig. 4 correspond to traverses through the ODF sections in Fig. 5. These sections were chosen amongst others because they contain the maximum positions in the three dimensional ODF space. Note that GRAN 133 is characterized by two maximum positions in the ODF, 60° apart in PSI 2, indicating that quartz is essentially hexagonal in those properties which concern the texture-forming mechanisms. For CC 627 there are two equal maxima at $\text{PHI} = 0$ which become unequal with increasing angle PHI.

Figure 6 presents separate pole figures for positive and negative rhombs (1011) and (0111) calculated from the ODF. These pole figures which cannot be measured separately illustrate more directly that GAE 9 strongly discriminates between positive and negative forms, in contrast to GRAN 133. Specimen CC 627 has a tendency for one maximum position of poles to *r* to lie at the margin of the pole figure, 90° away from the *a*-axis maximum of Fig. 3c.

Figure 7 illustrates the textures of specimen CC 550. The fact that the majority of *c*-axes lie on a girdle oblique in the sense opposite to the sense of shear illustrates that the sign of obliquity of a *c*-axis pole figure does not relate in a simple manner to the shear sense. The pole figure for *c* shows a weakly developed second girdle with the same sense of deflection from the fabric axes as found in CC 627.

Figure 8 expresses the probability of finding a particular crystal direction aligned with the foliation normal in the form of inverse pole figures. It has to be emphasized that inverse pole figures for specimens without an axially symmetric texture only provide incomplete information. Only for axially symmetric textures, found in many of the experimentally deformed specimens, do the inverse pole figures provide complete information and are therefore to be preferred over ordinary pole figures. Here the inverse pole figures are merely presented in order to show more readily the following features: GAE 9 and GRAN 133 differ in that the foliation normal of GAE 9 shows a strong tendency to prefer the crystal *a*-direction over the pole to *m*. CC 627 and CC 550 differ mainly in respect to the probabilities of finding a foliation normal aligned with a positive rhomb *r* and with both prisms *a* and *m*.

The main differences between CC 627 and CC 550, collected in the same area and deformed with the same sense of shear relative to the chosen projections are best characterized in the form of Figs. 9 and 10, showing the

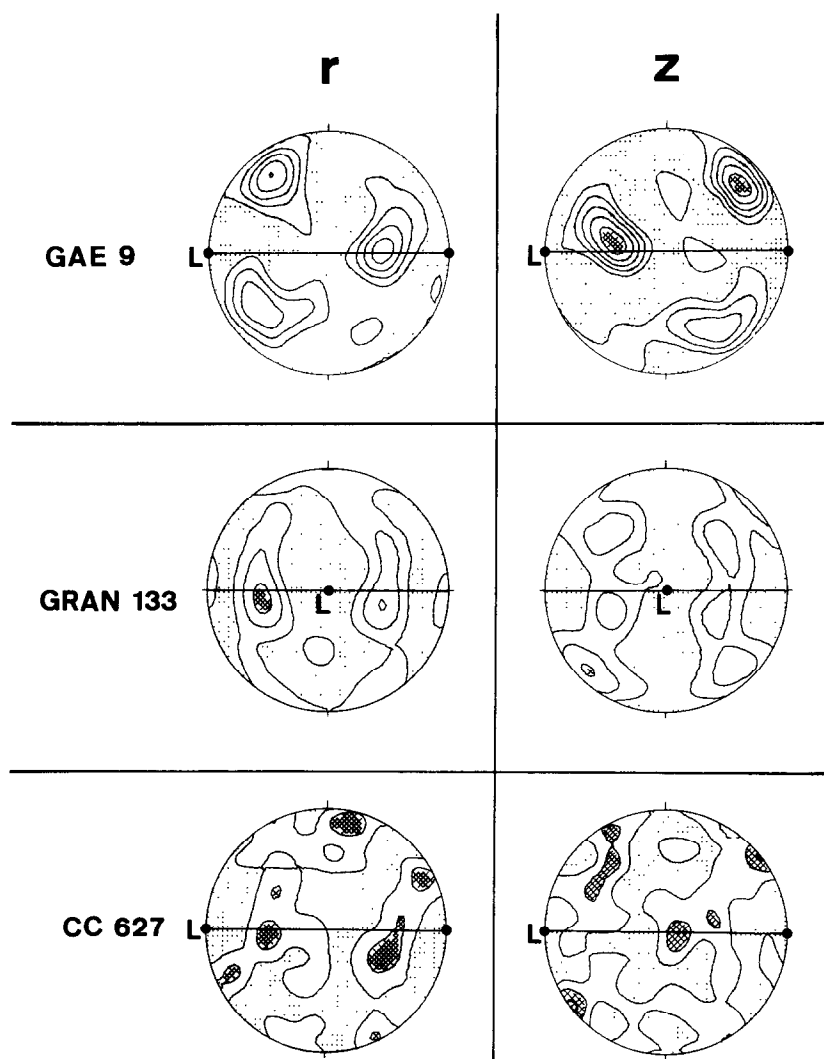


Fig. 6. Pole figures for r ($10\bar{1}1$) and z ($01\bar{1}1$) for the same specimens presented in Figs. 3–5, calculated from the ODF, order of expansion 12. Contour intervals in 1.0 of a uniform distribution, equal area projection, stippled areas with a density < 1.0 .

favoured crystal positions in the specimen coordinate frame: in specimen CC 627 the crystals with a c -axis parallel to either c -axis maxima in Fig. 3c, have a tendency for a pole to r to lie near the foliation normal and for a common a pole near the lineation (Fig. 9a). Crystals with a c -axis in the centre of the pole figure (Fig. 9b) again tend to have an a pole near the lineation but the probabilities of finding the foliation normal subparallel to a positive or negative rhomb is equal, see Fig. 9b and compare Fig. 4, e .

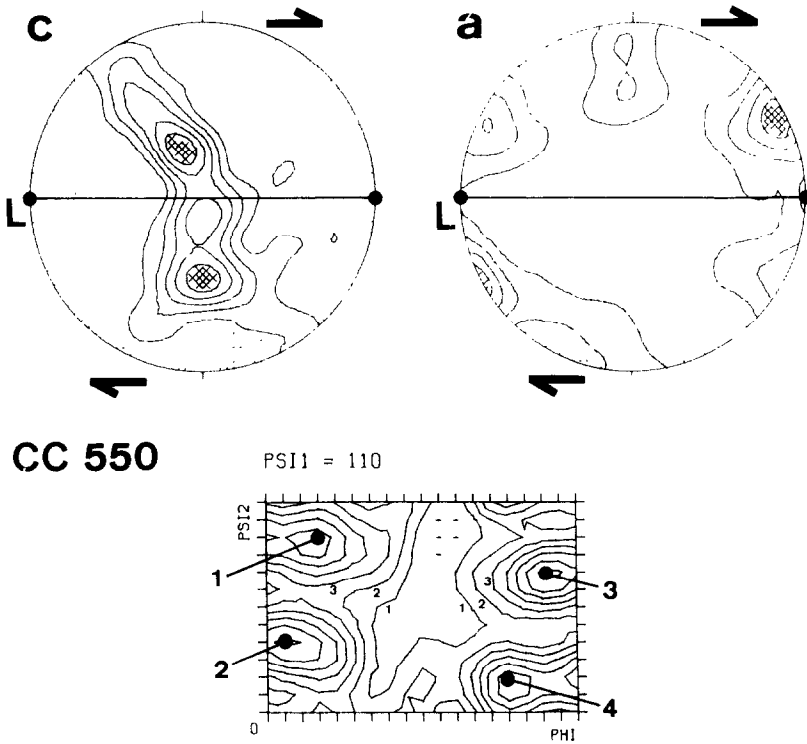


Fig. 7. Top: pole figures for *c* and *a* ($11\bar{2}0$) for specimen CC 550, calculated from the ODF, order of expansion 12. Contour intervals in 1.0 of a uniform distribution, equal area projection, stippled areas with a density < 1.0 . Bottom: selected section through the ODF of specimen CC 550, order of expansion 8. Dashes: negative probabilities.

For specimen CC 550 four different *c*-axis positions were chosen, corresponding to the maximum positions in the ODF section of Fig. 7 (Fig. 10a). Positive and negative forms are interchangeable to some extent, but as an *r* pole is rotated by 60° around *c* the most favoured position of *c* changes its position slightly (from positions 1 and 4 to positions 2 and 3 respectively on

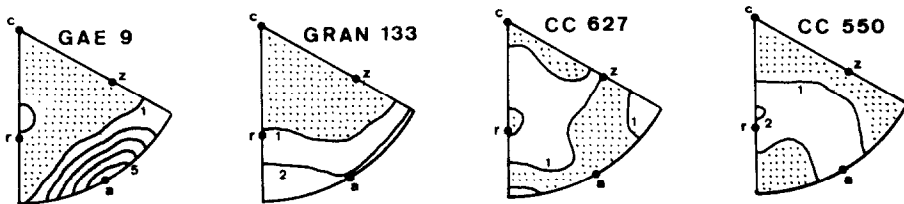


Fig. 8. Inverse pole figures for the foliation normal, calculated from the ODF, order of expansion 12, equal area projection.

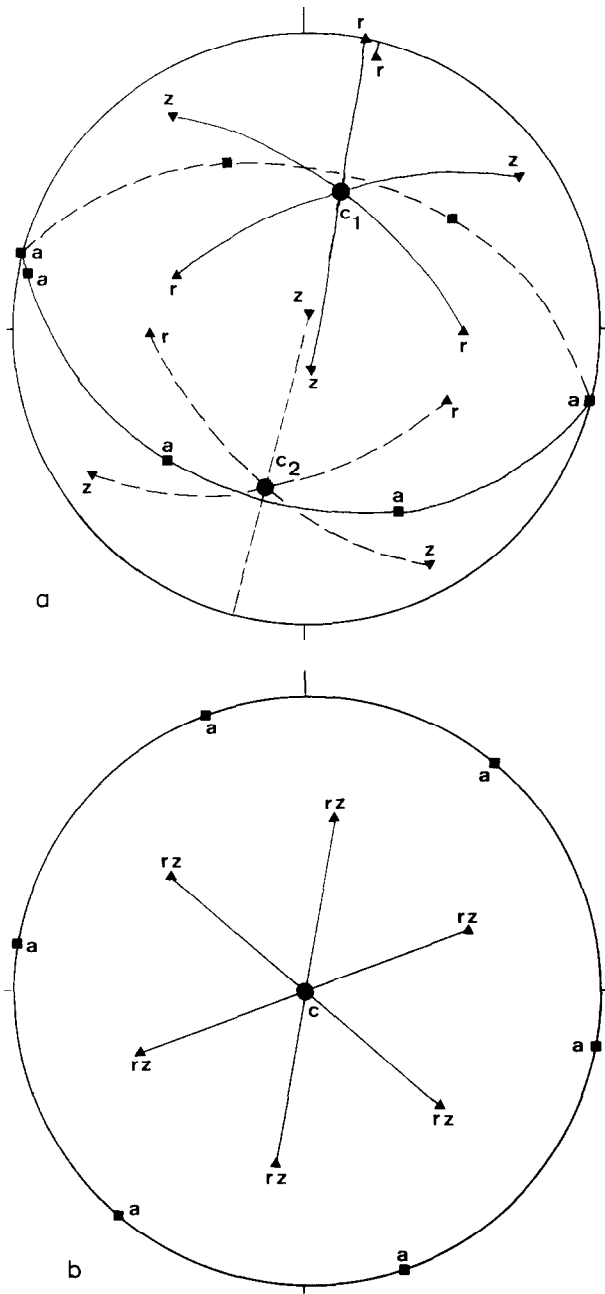


Fig. 9. Favoured crystal orientations for specimen CC 627 in the coordinate frame of the pole figures of Fig. 3. The c -axis positions labelled c_1 and c_2 in Fig. 9a correspond to the positions labelled 4c and 4d in Fig. 3c. Fig. 9b refers to the favoured crystal orientation of grains with their c -axis in the centre of the pole figure of Fig. 3c.

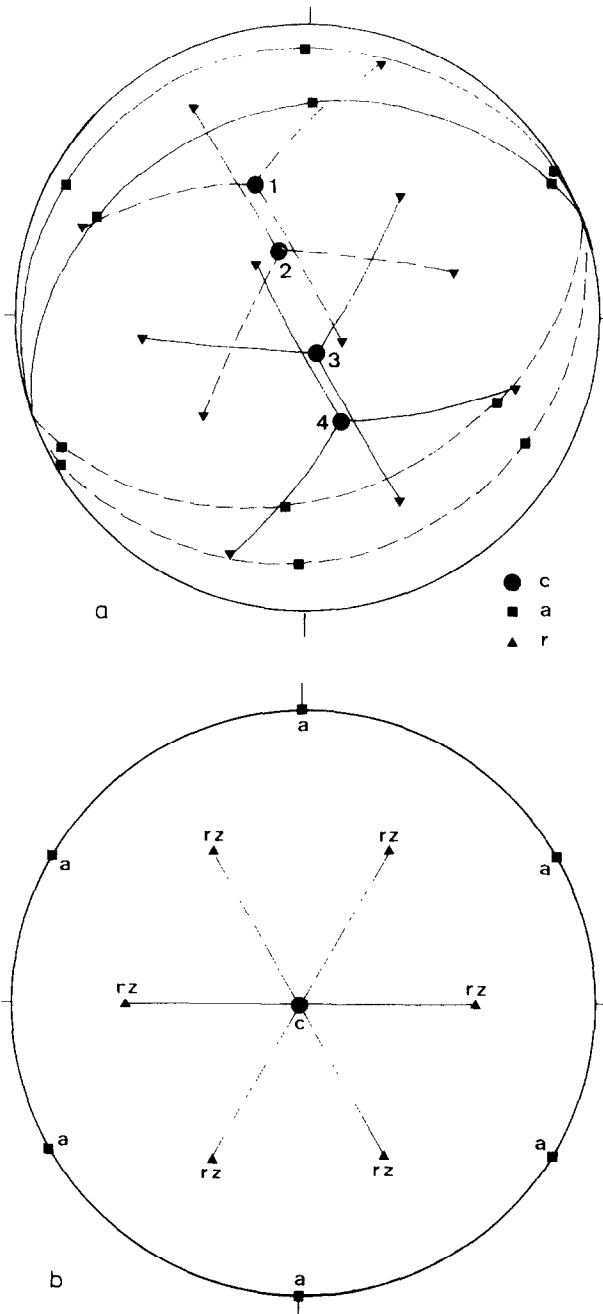


Fig. 10. Favoured crystal orientations for specimen CC 550 in the coordinate frame of the pole figures of Fig. 7. The *c*-axis positions labelled 1–4 in Fig. 10a refer to the positions in the ODF section of Fig. 7, labelled 1–4. Figure 10b refers to the favoured crystal orientation of grains with their *c*-axis in the centre of the pole figure of Fig. 7.

Fig. 10a). All four positions have an a -axis near the pole to the c -axis great circle girdle defined by the c -axis positions 1–4. Similar favoured crystal positions are found for the weakly developed crossed girdle of c -axes (Fig. 7), but now these crystal positions are mirror symmetric about a N–S mirror plane perpendicular to the projection plane of Fig. 10. Figure 10b shows that r and z are interchangeable for c -axis positions at the centre of the pole figure. In contrast to Fig. 9b the symmetry axes of this ideal crystal position coincide with the macroscopic fabric axes. Thus, some components of the texture in CC 550 have symmetry planes coinciding with the macroscopic fabric axes.

DISCUSSION

An intermediate aim of texture analyses is the identification of the operative glide systems. Once this difficult task is achieved it becomes easier to infer the conditions of deformation (temperature, strain rate, stress etc.) and important information on the deformation path (kinematic analysis). The results presented in the previous section illustrated that a large amount of additional information, not contained in a c -axis pole figure alone, can be obtained by a complete texture analysis.

Before we discuss the role of intracrystalline glide systems in the development of the texture we have to discuss the influence of Dauphinée twinning which has been demonstrated to have an effect on the preferred orientation of positive and negative forms in quartz aggregates experimentally deformed at high differential stresses (Tullis and Tullis, 1972). These experiments convincingly indicate that differences in elastic strain energy at high stresses can induce a concentration of positive rhombs r parallel to the principal axis of compression at the expense of negative forms by the operation of Dauphinée twinning involving a 180° rotation of the twinned portion of the crystal around the c -axis (corresponding to a 60° rotation in an inverse pole figure representation confined to a 60° portion of the crystal projection). Baker and Riekels (1977) attempted to interpret the texture of a quartz mylonite in terms of Dauphinée twinning, concluding that the effects of Dauphinée twinning correlate with total strain rather than stress and elastic strain. This conclusion is difficult to understand in view of the fact that Dauphinée twinning produces negligible permanent strain.

In specimen GRAN 133 Dauphinée twinning certainly had no effect on the texture because positive and negative forms have been shown to have the same orientation distribution. In the case of GAE 9, however, it could be argued that the effect of elastic strains caused the asymmetry in the intensity profile along a rotation around PSI 2 of Fig. 4a. The existence of a second but weaker peak exactly 60° away from the main peak in Fig. 4a tends to oppose such an interpretation because we would expect a trough in this position, due to the highest efficiency of twinning at 60° away from the main peak. For specimens CC 627 and CC 550 we demonstrated a strong interdependence of the preferred orientation of positive and negative forms

with all the other elements of the texture. This suggests that the texture has formed in response to a single and internally consistent mechanism of texture formation rather than by the superimposition of texture elements caused by glide with other elements caused by Dauphinée twinning.

This evidence against a substantial role of Dauphinée twinning in texture formation of the specimens studied here can be reconciled with the findings of Tullis and Tullis (1972), that the effect of Dauphinée twinning decreased with decreasing stresses whereas the duration of the exposure to stress had no great effect. It is likely that the differential stresses during natural deformation were lower than the range of stresses applied in these experiments (2–16 kb).

If Dauphinée twinning can be ruled out for specimen GAE 9 it has to be concluded that glide systems other than basal and prismatic glide must have been active, although the good alignment of the second order prisms a with the foliation and the c -axis with the stretching lineation suggest that glide on a in the direction of c was important. This glide system is well documented as active in experimentally deformed synthetic quartz (e.g. Kirby and McCormick, 1979). The additional preferred orientation of positive and negative forms would demand that the resistance to glide on equivalent positive and negative forms, also active during deformation of this specimen, was unequal.

In the case of GRAN 133 deformation in the stability field of β quartz cannot be ruled out in view of the "hexagonal" character of the texture. Such a possibility was considered by Starkey (1979) who analyzed the same specimen with an X-ray camera method. Deformation in the high temperature stability field is feasible since this specimen was collected in the neighbourhood of a basic intrusion (Behr 1965). If the specimen deformed in the α field we would have to conclude either that basal and prismatic glide alone were operative or that there was equal resistance to glide along positive and negative forms. It is interesting to note here that Bunge and Wenk (1977) described a remarkably similar texture for their specimen 293 collected in the highly metamorphic Gruf complex near the intrusion of the Bergell batholith of the Swiss Alps.

For specimen CC 627 field evidence puts additional constraints on the deformation path which certainly had a strong component of dextral shear. Eisbacher (1970), Bouchez and Pécher (1976) and subsequently many others described c -axis pole figures with the same sense of obliquity as in this specimen with respect to the sense of shear. The complete description of the texture of a quartzite from the main central thrust of the Himalayas by Bouchez et al. (1979) shows that there is a remarkable similarity between their specimen 620 and CC 627 in regard to all the measured pole figures. Assuming that the texture of specimen CC 627 represents stable end orientations in simple shear it is tempting to interpret the obliquity of this texture by invoking (1) glide on the positive rhomb r with a as the glide direction and (2) a tendency to orient a single dominant glide plane and direction in individual grains close to the shear plane and shear direction of the bulk deformation.

This interpretation is similar to the one given by Bouchez et al. (1979) for their specimen, based on the work of Etchecopar (1977), with the exception that these authors invoke basal glide parallel to a . For those grains in specimen CC 627 with their c -axis parallel to the intermediate strain axis glide on the first order prism m parallel to a could have been active. Both these glide systems are compatible with the result of TEM work by White et al. (1978) on the Cap de Creus material.

An interpretation for specimen CC 550 which came from the same area is more difficult. The fact that some components of the texture in this specimen have symmetry planes coinciding with the macroscopic fabric axes, opens the possibility of a deformation path which was more complex than just simple shear or that the concept of a stable end orientation should not be applied in the case of this specimen. Certainly an attempt to infer the sense of shear from the texture would be difficult in the case of this specimen.

Specimen CC 627 and to a minor extent also CC 550 are characterized by a very definite tendency for the crystal a -directions to be strongly aligned. In view of the fact that the shortest possible Burgers vector for quartz coincides with the a -direction we suggest that there may be dislocation interactions between grains such that the passage of dislocations with a Burgers vector parallel to a from grain to grain is facilitated when adjacent grains have parallel a -directions. This in turn could produce work softening during texture formation in the shear zone.

This discussion has illustrated the complexity of texture interpretation even after a complete texture analysis and that none of the interpretations presented here could be based on a c -axis pole figure alone. By increasing the number of complete texture analyses and by gaining further restraints from complementary field and microstructural studies, from computer simulations and from experimental work it is expected that the difficulties in interpreting texture data will be overcome.

CONCLUSIONS

(1) X-ray texture analyses are not restricted to the study of fine-grained monomineralic rocks. Polyminerallc specimens as well as coarse-grained specimens can yield good results.

(2) Dauphiné twinning is not considered to be an important texture forming mechanism at geological stress levels.

(3) Positive and negative glide systems in quartz can have different resistances to glide.

(4) The a -direction is an important glide direction in the Cap de Creus material and dislocation interactions from grain to grain may occur.

(5) Care must be exercised in using the obliquity in both c and a pole figures to infer the sense of shear.

(6) Complete texture descriptions are an essential element in understanding texture formation but need complementary studies to yield their full

potential. At present *c*-axis pole figures do not provide enough information for texture interpretation.

ACKNOWLEDGEMENTS

We thank Ph. Matte, A. Garcia and H.J. Behr for providing us with specimens. H.J. Möck developed the software used for automatic texture measurements. F. Pirovino and U. Gerber helped in specimen preparation and photographic reproduction, respectively. For stimulating discussions we thank A. Garcia, G. Lister, C. Simpson and S. White. J.G. Ramsay encouraged research in texture measurements and made the visits of two of us (M.C. and J.S.) to ETH Zürich possible. M.C. wishes to thank the Royal Society for financial assistance.

REFERENCES

- Baker, D.W. and Wenk, H.P., 1972. Preferred orientation in a low symmetry quartz mylonite. *J. Geol.*, 80: 81–105.
- Baker, D.W. and Riekels, L.M., 1977. Dauphinée twinning in quartzite mylonite. *J. Geol.*, 85: 15–26.
- Behr, H.J., 1961. Beiträge zur petrographischen und tektonischen Analyse des sächsischen Granulitgebirges. *Freib. Forschungsh.*, Reihe C, 119: 1–146.
- Behr, H.J., 1965. Zur Methodik tektonischer Forschung im kristallinen Grundgebirge. *Ber. Geol. Ges. DDR*, 10: 163–179.
- Bouchez, J.L. and Pécher, A., 1976. Plasticité du quartz et sens de cisaillement dans des quartzites du grand chevauchement central himalayen. *Bull. Soc. Géol. Fr.*, 6: 1377–1385.
- Bouchez, J.L., Dervin, P., Mardon J.P. and Englander M., 1979. La diffraction neutronique appliquée à l'étude de l'orientation préférentielle de réseau dans les quartzites. *Bull. Minéral.*, 102: 225–231.
- Bunge, H.J., 1969. *Mathematische Methoden der Texturanalyse*. Akademie-Verlag, Berlin, 330 pp.
- Bunge, H.J. and Wenk, H.R., 1977. Three-dimensional texture analysis of three quartzites (trigonal crystal and triclinic specimen symmetry). *Tectonophysics*, 40: 257–285.
- Carreras, J., Estrada, A. and White S., 1977. The effects of folding on the *c*-axis fabrics of a quartz mylonite. *Tectonophysics*, 39: 3–24.
- Casey, M., 1981. Numerical analysis of X-ray texture data: An implementation in Fortran allowing triclinic or axial specimen symmetry and most crystal symmetries. *Tectonophysics*, 78: 51–64.
- Eisbacher, G.H., 1970. Deformation mechanisms of mylonite rocks and fractured granites in Cobequid Mountains, Nova Scotia, Canada. *Geol. Soc. Am. Bull.*, 81: 2009–2020.
- Etchecopar, A., 1977. A plane kinematic model of progressive deformation in a polycrystalline aggregate. *Tectonophysics*, 39: 121–139.
- Kerrich, R. and Starkey, J., 1979. Chemical removal of feldspar and layer silicates from quartz-bearing rocks for X-ray petrofabric studies. *Am. Mineral.*, 64: 452.
- Kirby, S.H. and McCormick, J.W., 1979. Creep of hydrolytically weakened synthetic quartz crystals oriented to promote $\{2\bar{1}10\} < 0001 >$ slip: a brief summary of work to date. *Bull. Minéral.*, 102: 124–137.
- Lister, G.S., Paterson, M.S. and Hobbs, B.E., 1978. The simulation of fabric development in plastic deformation and its application to quartzite: the model. *Tectonophysics*, 45: 107–158.

- Matte, Ph., 1968. La structure de la virgation hercynienne de Galice (Espagne). Extrait Trav. Lab. Géol. Fac. Sci. Grenoble, tome 44.
- Riekels, L.M. and Baker, D.W., 1977. The origin of the double maximum pattern of optic axes in quartzite mylonite. *J. Geol.*, 85: 1–14.
- Schmid, S.M., Casey, M. and Starkey, J., 1981. The microfabric of calcite tectonites from the Helvetic nappes (Swiss Alps). *Geol. Soc. London, Spec. Publ.*, in press.
- Siddans, A.W.B., 1976. Deformed rocks and their textures. *Philos. Trans. R. Soc. London, Ser. A*, 283: 43–54.
- Smith, G.S. and Alexander, L.E., 1963. Refinement of the atomic parameters of α -quartz. *Acta Crystallogr.*, 16: 462–471.
- Starkey, J., 1979. Petrofabric analyses of Saxony granulites by optical and X-ray diffraction methods. *Tectonophysics*, 58: 201–219.
- Tullis, J. and Tullis, T., 1972. Preferred orientation of quartz produced by mechanical Dauphinée twinning: thermodynamics and axial experiments. *Am. Geophys. Union, Geophys. Monogr.*, 16: 67–82.
- White, S.H., Burrows, S.E. and Carreras, J., 1978. Textural and microstructural development in a naturally deformed quartzite: a metallurgical approach. *Proc. 5th ICOTOM*, 2: 211–220, Springer, Berlin.